CHIN. PHYS. LETT. Vol. 37, No. 8 (2020) 087301

Anisotropy Properties of Mn_2P Single Crystals with Antiferromagnetic Transition

Shi-Hang Na(那世航)[1,2], Wei Wu(吴伟)[1,2*], and Jian-Lin Luo(雒建林)[1,2,3*]

[1]*Beijing National Laboratory for Condensed Matter Physics and Institute of Physics, Chinese Academy of Sciences, Beijing 100190, China*

[2]*School of Physical Sciences, University of Chinese Academy of Sciences, Beijing 100190, China*

[3]*Songshan Lake Materials Laboratory, Dongguan 523808, China*

(Received 19 May 2020; accepted 18 June 2020; published online 28 July 2020)

Single crystals of hexagonal structure Mn_2P are synthesized by Sn flux for the first time. Transport and magnetic properties have been performed on the single crystals, which is an antiferromagnet with Neel temperature 103 K. Obvious anisotropy of resistivity is observed below the Neel temperature, which is manifested by metallic behavior with a current along the c-axis and semiconducting behavior with a current along the a-axis. The negative slope of temperature-dependent resistivity is observed above the Neel temperature in both a and c directions. Strong anisotropy of magnetic susceptibility is also evident from the magnetization measurements. A weak metamagnetic transition is observed only in a-axis plane at high magnetic field near 50–60 K compared to the c-axis. We believe these strong anisotropies of magnetic and transport properties are due to the anisotropy of spin arrangement. Mn_2P could be a candidate for exploration of possible superconductivity due to the low spin state.

PACS: 73.20.−r, 71.27.+a, 74.70.Xa DOI: 10.1088/0256-307X/37/8/087301

Since the discovery of superconductivity in CrAs and MnP under pressure, great efforts have been made to explore Cr or Mn-based systems in metal pnictides and oxides.[1−7] Superconductivity in MnP single crystal under pressure was discovered in 2015, which is the first Mn-based superconductor.[3] MnP undergoes a ferromagnetic transition at $T_c \approx 290$ K and antiferromagnetic transition with a double helical spin structure at $T_N \approx 55$ K. Bulk superconductivity with $T_c \approx 1$ K emerges at about 8 GPa, where the magnetic order is completely suppressed. Several experiments including NMR, μSR neutron scattering and magnetic x-ray diffraction for MnP revealed that there are complex magnetic transformations under high pressure.[8−11] The low spin state of $1.3\mu_B$ and the high quality of the single crystal are important conditions for the discovery of superconductivity in MnP under pressure. To date, MnP is the only superconductor in Mn-based materials, thus it is of great interest to study other Mn-based materials with magnetism.

We spotlighted phosphide Mn_2P with $C22$ hexagonal structure (space group $P62m$, $a = 6.081$ Å, $c = 3.460$ Å), whose properties have not been investigated sufficiently so far.[12−16] An earlier neutron diffraction study of polycrystalline samples shows that Mn_2P materials contain two kinds of Mn atoms, Mn(1) and Mn(2), as shown in Fig. 1. Mn(1) is surrounded by four phosphorus atoms in a distorted tetrahedron and Mn(2) is surrounded by five P atoms in a square-based pyramid. Mn_2P is an antiferromagnet with Neel temperature 103 K. Two of the three Mn(2) have a magnetic moment of $0.84(3)\mu_B$, two of the three Mn(1) have one of $0.01(4)\mu_B$ and the third Mn(1) and Mn(2) have no moments. All directions of moments are strictly along the a-axis.[16]

In this letter, we for the first time synthesized high-quality Mn_2P single crystals grown by the Sn flux method and observed a strong anisotropy of transport and magnetic properties in the single crystals. Obvious anisotropy of resistivity is detected below the Neel temperature with a metallic behavior with a current along c-axis while a semiconducting behavior with a current along the a-axis, the magnetically easy axis. This strongly anisotropy in resistivity is due to the scattering of the conducting electrons by localized moments with anisotropic spin arrangement. Negative slope of temperature-dependent resistivity is observed above the Neel temperature in both directions. The magnetic susceptibility anisotropy is also evident from the magnetization measurements. A weak metamagnetic transition in a-axis plane at high magnetic field near 50–60 K is ascribed to the spin reorientation along the a-axis plane other than along the c-axis. In addition, the electronic specific-heat coefficient is obtained to be about $20\,\mathrm{mJ\cdot K^{-2}\cdot mol^{-1}}$. The high qual-

Supported by the National Key Research and Development of China (Grant No. 2017YFA0302901), the National Natural Science Foundation of China (Grant Nos. 11674375, 11634015 and 11921004), the Strategic Priority Research Program of the Chinese Academy of Sciences (Grant No. XDB33010100), and the Postdoctoral Science Foundation of China.

*Corresponding authors. Email: welyman@iphy.ac.cn; jlluo@iphy.ac.cn

© 2020 Chinese Physical Society and IOP Publishing Ltd

ity of single crystal and relatively low spin state make Mn_2P a good candidate for exploring the possible superconductivity once the AFM phase is suppressed by either doping or high pressure.

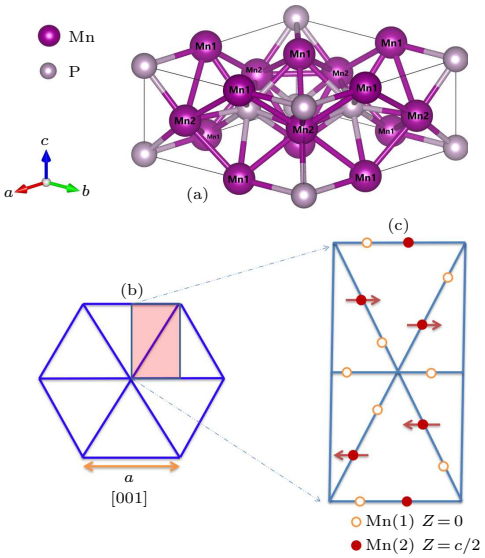

Fig. 1. (a) The crystal structure of Mn_2P. (b) The [001] projections of crystal unit cell of Mn_2P. (c) The [001] projections of magnetic structure of orthorhombic cell of Mn_2P.

Mn_2P crystals were grown using the Sn-flux method. The starting materials were Mn (Cerac, powder, 99.95%), P (Alfa Aesar, powder, 99.999%), and Sn (Cerac, shot, 99.999%). All of the manipulations were carried out in an argon-filled glove box with moisture and oxygen levels less than 1 ppm. The materials with atomic ratio of Mn:P:Sn = 2:1:40 were added to an alumina crucible, which was placed in a quartz ampoule, and subsequently sealed under a reduced pressure of 10^{-4} Torr. The quartz ampoule was heated up to 650 ℃ for 20 h, held there for a period of 8 h, then heated up to 1000 ℃ for 15 h, held for 6 h, and slowly cooled down to 600 ℃ for 50 h. At this temperature, liquid Sn flux was filtered by centrifugation. The resulting products were metallic needle-shaped black crystals with dimensions up to $0.3 \times 0.3 \times 2\,\text{mm}^3$. The crystals were grown along the c-axis and they are stable in air and water.

Energy-dispersive x-ray (EDX) analysis on these crystals was carried out using a Hitachi S-2700 scanning electron microscope. The results show that the chemical compositions are 67(2)% Mn and 33(2)% P. No Sn elements were detected in the crystals analyzed. The magnetic susceptibility was measured in the temperature range of 2–300 K using a SQUID VSM Magnetometer of Quantum Design Company. The resistivity was measured between 2 and 300 K by the standard four-probe method in a PPMS system of the Quantum Design company. The current was applied along the c-axis and a-axis of the crystal.

Figure 2 shows the XRD in single crystal of Mn_2P under ambient conditions, which indicates that Mn_2P crystallized in hexagonal structure with space group $P62m$. The [100] series reflections can be well indexed based on a hexagonal cell with lattice parameter $a = 6.082$ Å, $c = 3.461$ Å, respectively, which are consistent with those reported in the literature ($a = 6.081$ Å, $c = 3.460$ Å).[16]

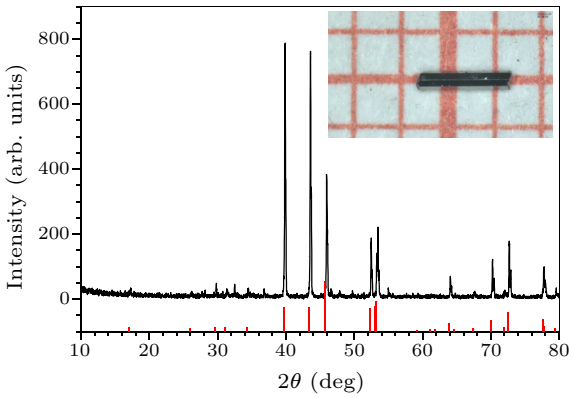

Fig. 2. X-ray diffraction patterns of an Mn_2P single crystal. The XRD patterns are well indexed on the base of the hexagonal structure with the space group $P62m$ with lattice parameters $a = 6.082$ Å, $c = 3.461$ Å, respectively. The inset is the picture of single crystal Mn_2P.

Figure 3 shows the temperature-dependent resistivity for Mn_2P from 1.8 K to 300 K at zero field with current I along c-axis and a-axis, respectively. Strikingly, an obvious kink is observed along both the directions at the Neel temperature of 103 K, which is the antiferromagnetic phase transition temperature. Below this temperature, the resistivity shows a metallic behavior with a current along the c-axis while a semiconducting behavior with current along the a-axis. We believe this strong anisotropy of resistivity is due to the scattering of conducting electrons with anisotropic spin formation of localized moments. Because all spins of Mn(2) are strictly pointing to the a-axis and the spins are parallel with neighboring ones along the c-axis, the scattering of conduction electrons by localized moments is relatively small, then a metallic behavior is observed along the c-axis direction. However, the spins are antiparallel with neighboring ones along the a-axis, the scattering of conduction electrons with unparallel localized moments is much larger than that in c-axis, thus a semiconducting behavior is observed in a-axis transport. The negative slope of temperature-dependent resistivity is observed in both directions above the Neel temperature. This indicates that the electron correlations are possibly related to Kondo scattering of a set of localized Mn d electron moments interacting with conduction electrons in the paramagnetic state or has a narrow gap in the high temperature. The detail of band structure information needs to be calculated in future to clarify this.

These results strongly indicate that Mn_2P contains a magnetic constituent with anisotropic geometry, leading to the anisotropic electrical transport governed by spin-associated scattering. The a-axis resistivity has a downturn below 30 K. It is probably due to the reasons that the crystal is not aligned properly and c-axis signal of resistance is mixed.

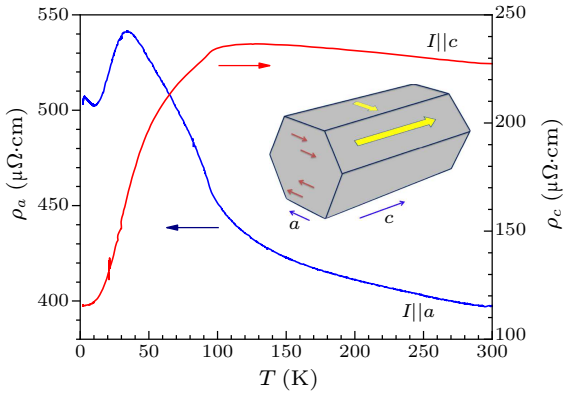

Fig. 3. Anisotropic resistivity of the Mn_2P single crystal for $I||c$ and $I\perp c$.

Magnetic magnetization M measurements were carried out at various magnetic fields for Mn_2P. Figure 4 shows the magnetic susceptibility $\chi = M/H$ as a function of temperature in a field of 1 T applied both parallel and perpendicular to the c-axis. Below 103 K, χ drops sharply in perpendicular to the c-axis, indicating a long-range order magnetic transition from a paramagnetic state to an AFM state. For $H||c$, the drop of χ is not so obvious because all the spins of Mn(2) in the AFM state are strictly along the a-axis with zero projection in the c-axis.

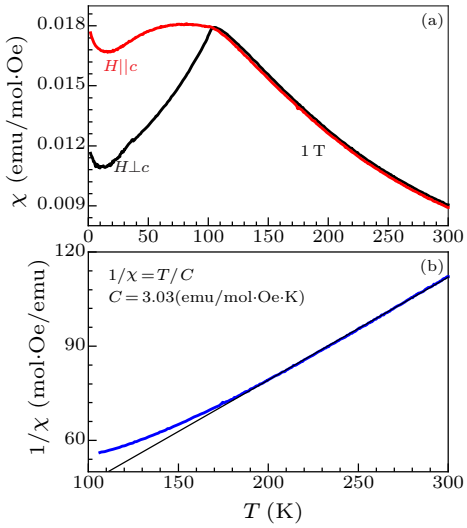

Fig. 4. (a) Anisotropic magnetic susceptibility χ versus temperature for $H||c$ and $H\perp c$ at field 1 T. (b) Reciprocal of magnetic susceptibility χ versus temperature.

At high temperatures, χ increases with decreasing T, showing Curie–Weiss-like behavior. This is in strong contrast to the parent compounds of iron pnictide superconductors where susceptibility decreases linearly with decreasing T above the SDW temperature. Using the Curie–Weiss law, we can estimate the effect magnetic moments to be $\mu_{\rm eff} = 4.89\mu_{\rm B}$, which is very close to $4.9\mu_{\rm B}$ that is the theoretical prediction of the moment for Mn^{3+} ions.

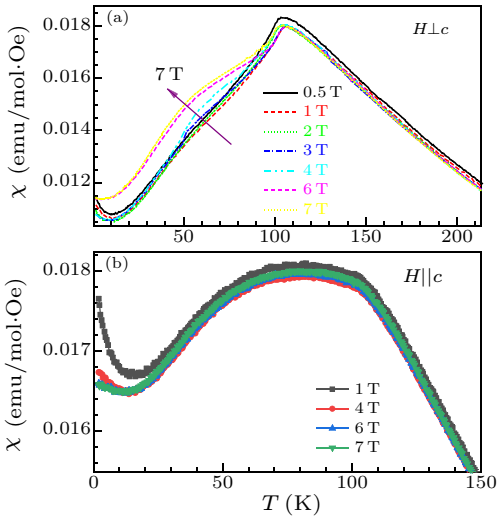

Fig. 5. (a) Anisotropic magnetic susceptibility χ versus temperature for $H||c$ and $H\perp c$ at different fields. (b) Field dependent resistivity measurements at different temperatures.

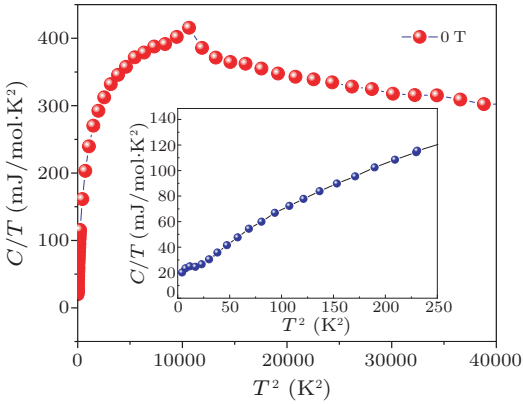

Fig. 6. Temperature dependence of normalized electronic specific heat C_e/T. The inset is the electronic specific heat of Mn_2P.

Figure 5 shows the magnetic susceptibility as a function of temperature in different fields applied both parallel and perpendicular to the c-axis. An obvious "shoulder" appears near 50 K when $H > 4$ T for the magnetic field perpendicular to the c direction. This is a weak field-induced metamagnetic transition due to spin reorientation or spin rearrangement in the a-axis. With increasing magnetic field, the shoulder becomes more apparent. The transition is likely due to a field-induced spin flip or spin flop transition at this temperature. A similar transition was also found in MnP and $Ce_{12}Fe_{57.5}As_{41}$ at high fields.[17,18]

Figure 6 shows the T dependence of specific heat

C/T in zero field below 200 K. A specific heat peak is obvious at the magnetic transition temperature about 103 K. The electronic specific-heat coefficient γ is about 20 mJ·K^{-2}·mol^{-1}, consistent with the previous report.[14] It is larger than that of MnRuP ($\gamma \sim$ 13 mJ·K^{-2}·mol^{-1} (Ref. [19])) with the same hexagonal structure and MnP ($\gamma \sim 6$ mJ·K^{-2}·mol^{-1}). In a Fermi liquid system, γ is proportional to density of states at Fermi level as well as effective mass of electrons. The relatively large value of γ in Mn_2P indicates relatively strong electron correlations.

In conclusion, single crystals of Mn_2P are firstly grown by the Sn flux method. Strong anisotropy of transport and magnetic properties are observed in the single crystals of Mn_2P. Obvious anisotropy of resistivity is observed below the Neel temperature, which is manifested by metallic behavior with a current along the c-axis and semiconducting behavior with a current along the a-axis. The anisotropy of magnetic anisotropy is evident from the magnetization measurements. A weak metamagnetic transition at high magnetic field near 50–60 K is observed. In the paramagnetic rang, the resistivity along each axis decreases slightly with increasing temperature like Fe_2P.[20] This is possibly related to Kondo scattering of a set of localized Mn d electron moments interacting with conduction electrons in the paramagnetic state.

To date, MnP is only one Mn-based superconductor under high pressure.[2] Normally, the ordered moments in Mn-based magnets are relatively large, it is difficult to suppress magnetic order in Mn-based compounds by either chemical doping or the application of high pressure. The maximum ordered moment in Mn_2P is only 0.84μ_B and a high-quality crystal is now available, thus Mn_2P is a good candidate in which the AFM phase could be suppressed by either chemical doping or the application of high pressure to explore the possible superconductivity.

References

[1] Wu W, Cheng J G, Matsubayashi K, Kong P P, Lin F K, Jin C Q, Wang N L, Uwatoko Y and Luo J L 2014 *Nat. Commun.* **5** 5508

[2] Cheng J G, Matsubayashi K, Wu W, Sun J P, Lin F K, Luo J L, Uwatoko Y 2015 *Phys. Rev. Lett.* **114** 117001

[3] Cheng J G and Luo J L 2017 *J. Phys.: Condens. Matter* **29** 440301

[4] Bao J K, Liu J Y, Ma C W, Meng Z H, Tang Z T, Sun Y L, Zhai H F, Jiang H, Bai H, Feng C M, Xu Z A and Cao G H 2015 *Phys. Rev. X* **5** 011013

[5] Mu Q G, Ruan B B, Pan B J, Liu T, Yu J, Zhao K, Chen G F and Ren Z A 2017 *Phys. Rev. B* **96** 140504

[6] Wu W, Liu K, Li Y J, Yu Z H, Wu D S, Shao Y T, Na S H, Li G, Huang R Z, Xiang T and Luo J L 2020 *Natl. Sci. Rev.* **7** 21

[7] Li Y J, Wu W, Liu K, Yu Z H, Wu D S, Shao Y T, Na S H, Li G, Zheng P, Xiang T and Luo J L 2019 *Europhys. Lett.* **128** 67002

[8] Zheng P, Xu Y J, Wu W, Xu G, Lv J L, Lin F K, Wang P, Yang Y F and Luo J L 2017 *Sci. Rep.* **7** 14178

[9] Wang Y, Feng Y J, Cheng J G, Wu W, Luo J L and Rosenbaum T F 2016 *Nat. Commun.* **7** 13037

[10] Matsuda M, Ye F, Dissanayake S E, Cheng J G, Chi S, Ma J, Zhou H D, Yan J Q, Kasamatsu S, Sugino O, Kato T, Matsubayashi K, Okada T and Uwatoko Y 2016 *Phys. Rev. B* **93** 100405(R)

[11] Fan G Z, Zhao B, Wu W, Zheng P and Luo J L 2016 *Sci. China. Phys. Mech. Astron.* **59** 657403

[12] Ishidat S, Asano S and Ishidat J 1987 *J. Phys. F* **17** 475

[13] Haggstrijm L, Sjastrijm J and Ericsson T 1986 *J. Magn. Magn. Mater.* **60** 171

[14] Malik S K and Vijayaraghavan R 1968 *Phys. Lett. A* **28** 9

[15] Nagase S, Watanabe H and Shinohara T 1973 *J. Phys. Soc. Jpn.* **34** 908

[16] Yessik M 1968 *Philos. Mag.* **17** 623

[17] Komatsubara T and Suzuki T 1969 *J. Phys. Soc. Jpn.* **26** 208

[18] Wu W and Luo J L 2018 *Sci. Chin. Phys. Mech. Astron.* **61** 127407

[19] Wu W, Luo J L and Zhou J S 2020 *Field-induced phase transition and anisotropic magnetoresistance in helical magnetic order on MnRuP single crystals* (submitted to *Phys. Rev. B*)

[20] Fujii H, Hokabe T, Kamigaichi T and Okamoto T 1977 *J. Phys. Soc. Jpn.* **43** 41